Photoluminescence and stimulated emission from microcrystalline CsPbCl₃ films prepared by amorphous-to-crystalline transformation

S. Kondo,* K. Suzuki, and T. Saito

Research Center for Development of Far-Infrared Region, Fukui University, Bunkyo, Fukui 910-8507, Japan

H. Asada

Department of Applied Physics, Faculty of Engineering, Fukui University, Bunkyo, Fukui 910-8507, Japan

H. Nakagawa

Department of Electronics, Faculty of Engineering, Fukui University, Bunkyo, Fukui 910-8507, Japan

Highly excited photoluminescence of CsPbCl₃, which is known to be one of the most photoluminescent semiconductors, has been measured for thin films prepared by crystallization from the amorphous phase into microcrystalline/polycrystalline states. With the increase of excitation intensity, the microcrystalline state shows successive jumps of the dominant emission band, from a free-exciton band to its phonon replica and finally to a lowest-energy band originating from exciton-exciton inelastic collision. For the exciton-exciton porcess stimulated emission occurs at very low threshold excitation intensities of the order of $10 \ kW/cm^2$ at 77 K. At higher excitation intensities above $50 \ kW/cm^2$, single-path-light-amplification stimulated emission across the film thickness is observed suggesting a very large optical gain. The large-gain mechanism is attributable to giant oscillator strength effect characteristic of excitonic superradiance recently reported for films prepared in the same way.

I. INTRODUCTION

Semiconductor microcrystals have attracted much attention over the last two decades or more owing to mesoscopic enhancement of linear and nonlinear optical properties. Various efforts have been made to obtain microcrystals or nanodimensional particles according to the object of investigation. In the study of quantum size effect on excitons, which is one of the most attractive mesoscopic properties exhibited by nanodimensional particles, the particles are usually embedded in a glass or crystal matrix. Such a specimen has mostly been prepared by means of quenching of thermal equilibrium for phase separation of an eutectic mixture. The resulting nanoparticles necessarily have a size distribution, reflecting the phase equilibrium. Furthermore, the mole fraction of the particles is generally very small, typically of the order of 0.1 mol % or less. Preparation of a specimen containing nanoparticles of a definite size with a high concentration is not merely desirable for the basic research of their mesoscopic properties, but for their application studies.

On the other hand, it has been shown that many metal halide semiconductors such as silver,[1] thallium,[2] copper,[3] lead,[4] or cadmium[5] halides, including their mixed systems,[6] can be rendered amorphous by quench deposition yielding film samples. The amorphous films have a well-defined, characteristic crystallization temperature at which their absorption spectra drastically change in outline (for example, see Fig. 1, where the inset illustrates the trace of the change in optical density during slow heating at a rate of 1 K/min, revealing that the crystallization temperature is located at 302 K). The films, when crystallized at temperatures just above the crystallization temperature, are generally in a mi-crocrystalline state, and changes into polycrystalline state when they are subsequently annealed at higher temperatures. Many of the crystalline films produced via the amorphous phase, whether they are microcrystalline or polycrystalline in nature, show very high transmittance compared with poly-crystalline films directly deposited onto hot substrates. The microcrystalline films provide alternative, extremely densely nanoparticle-dispersed specimens of high quality for studying mesoscopic enhancement of optical properties.

Concerning CsPbCl₃, which is known to be one of the most photoluminescent semiconductors,[7] we recently reported[8] that high-quality films composed of crystallites with narrow size distributions are obtainable for various crystallite-size levels, from microcrystalline to polycrystalline, by crystallizing the amorphous films step by step in a controlled manner by means of shotlike IR laser light irradiation of the amorphous films using a CO₂ laser. Their photoluminescence is dominated by free-exciton emission at every size level without showing trapped-exciton emission, in great contrast to the case for bulk single crystals (whose photoluminescence spectrum is dominated by trapped-exciton emission related to defects in the crystals). The microcrystalline state shows extremely enhanced free-exciton emission as compared to the polycrystalline state, but with the latter state still showing stronger free exciton luminescence than bulk single crystals. The enhanced free-exciton emission in the microcrystalline state is attributed to the occurrence of excitonic superradiance in the microcrystallites. The excitonic superrradiance-induced enhancement factor, which is the ratio of integrated luminescence intensity for the microcrystalline state at optimal microcrystallite-size levels to that for the polycrystalline state, varies from film to film,
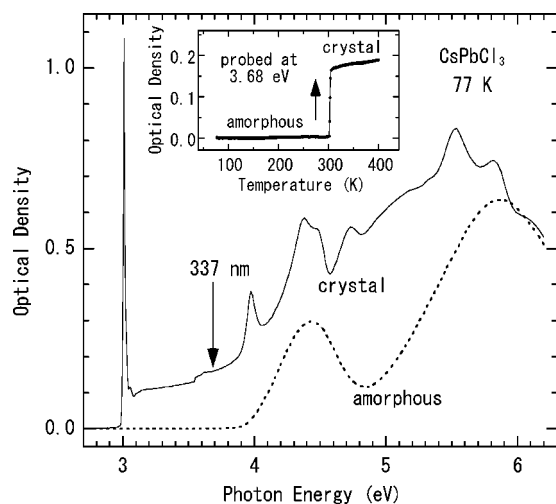
FIG. 1. The absorption spectra of $CsPbCl_3$ films at 77 K for the amorphous (dashed curve) and crystalline (solid curve) states. The downward arrow indicates the energy position of the N_2 laser light (337 nm) used in the present study of photoluminescence. The inset illustrates the change in optical density during crystallization

but always lies in the range from 5 to 20.[8] In the present paper we report subsequent studies of photoluminescence measured under high-power excitation. The luminescence spectra were very different in feature from those of bulk single crystals reported in Ref. 9, which is the only existing photoluminescence study of $CsPbCl_3$ under high-power excitation. It was found that the microcrystalline state of the films shows strongly enhanced stimulated emission, compared to the case for the polycrystalline state as well as the case for bulk single crystals.

II. EXPERIMENTAL

Microcrystalline/polycrystalline $CsPbCl_3$ films were prepared by the shotlike IR laser light irradiation method described in Ref. 8. In brief, amorphous $CsPbCl_3$ films, vacuum quench deposited onto silica-glass substrates attached to a copper block cooled to 77 K, were subjected to fast heating/cooling cycles by cw CO_2 laser light irradiation to achieve various microcrystalline/polycrystalline states stepwise; the irradiation time per cycle was in the range from 10 to 3000 ms depending on the desired crystallite-size levels. The size levels were monitored by *in situ* free-exciton emission spectroscopy. For this purpose photoluminescence under low-power excitation was intermittently measured (measurement time, 1 s) during the repeated heating/cooling cycles, using an exciting light of wavelength 380 nm from a monochromator (light source, 500-W Xe lamp). Crystallite sizes (effective sizes) were determined from the blueshift of the free-exciton energy relative to that for the polycrystalline state, in the same way as that employed, for example, in Ref. 10. After appropriate size levels were reached in the film, photoluminescence under high-power excitations was measured together with absorption spectrum. The high-power excitation was performed for various excitation intensities by using an N_2 laser (wavelength, 337.1 nm; power, 200 kW;
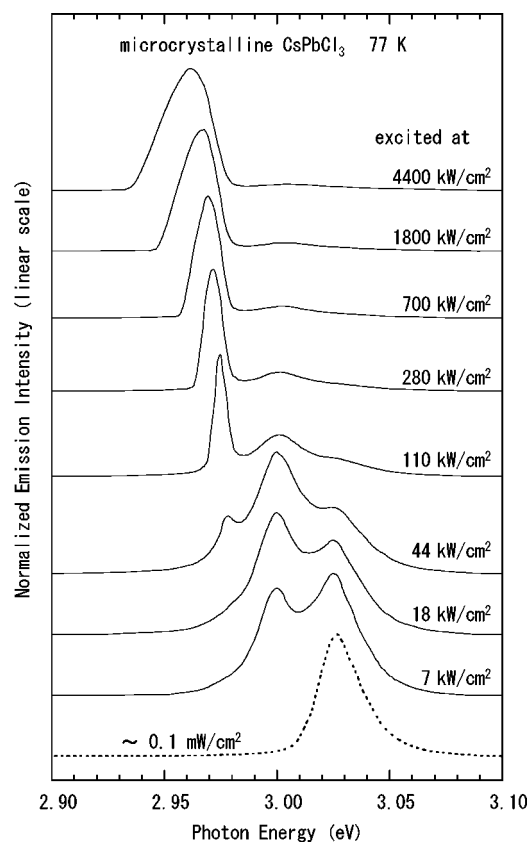

FIG. 2. Luminescence spectra for the microcrystalline state of a film of 82 nm thickness with an effective crystallite diameter of 4.0 nm, measured at 77 K for various excitation intensities indicated. The maximum intensities of the spectra are normalized to unity.

pulse duration, 0.5 ns) and a variable-reflectivity neutral density filter. All the measurements were carried out *in situ* on a liquid nitrogen-cooled CCD spectrometer with the help of fiber optics. The resolution of the spectrometer was set to 0.5 nm.

III. RESULTS

Figures 2 and 3 show luminescence spectra for the microcrystalline and polycrystalline states, respectively, of a film of 82 nm thickness, measured at 77 K for various excitation intensities indicated. The measurements were carried out in a configuration of back scattering normal to the film. The incident angle of the exciting light was 45° with respect to the film and its spot at the film surface had a dimension of about 2×2 mm^2. In the figures the maximum intensities of the spectra are normalized to unity. The dashed curves in the figure represent a free-exciton emission band measured under ordinary-light (wavelength, 380 nm) excitation. The integrated intensity of the band was shown to be 7.2 times larger for the microcrystalline state than for the polycrystalline state. The effective mean crystallite size for the microcrystalline state was about 4.0 nm in diameter (effective diameter), which was determined simply by comparing the observed blueshift 20 meV with the reported blueshift versus
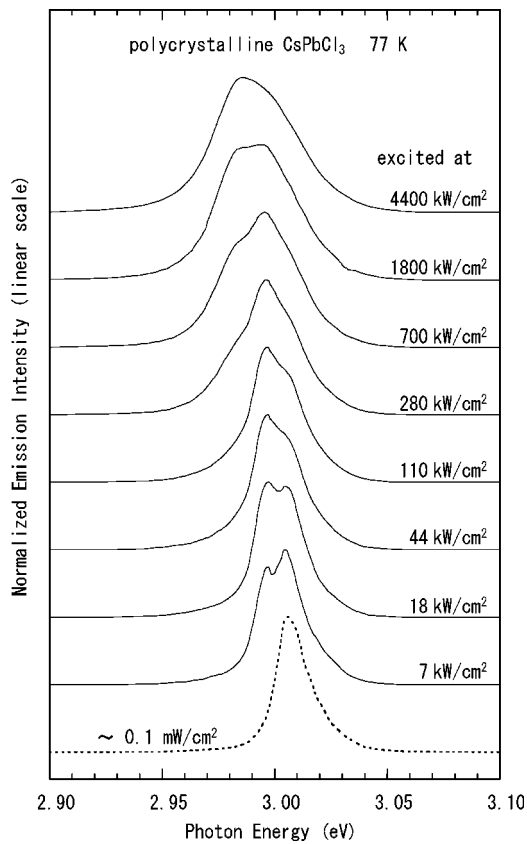
FIG. 3. Luminescence spectra for the polycrystalline state of a film of 82 nm thickness, measured at 77 K for various excitation intensities indicated. The maximum intensities of the spectra are normalized to unity.
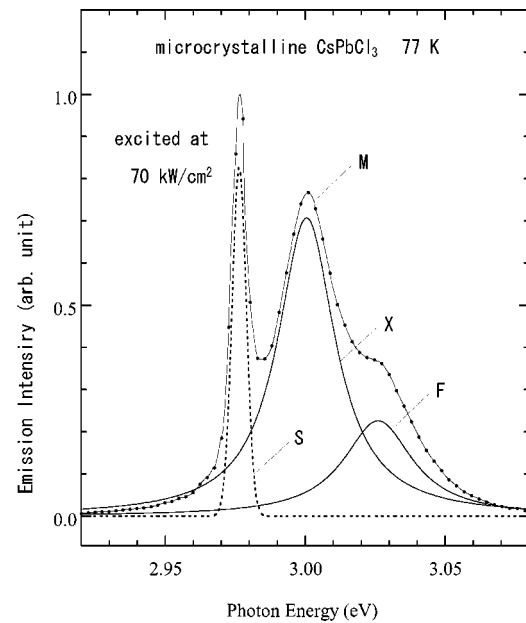

FIG. 4. An example of spectral analysis for the microcrystalline state (effective crystallite diameter, 4.0 nm): the measured luminescence spectrum M is decomposed into three bands, namely, F (Gaussian), X (Lorentzian), and S (Lorentzian) bands.

sured for various excitation intensities. The results are summarized in regard to integrated emission intensity (Fig. 5) and peak energy (Fig. 6) of the three bands, plotted against excitation intensity.

From the log-log plots (Fig. 5) of the integrated emission intensity I_{em} versus the excitation intensity I_{ex}, it is seen that the slope n involved in the expression $I_{em} \propto I_{ex^n}$ is in the

FIG. 5. Integrated emission intensity versus excitation intensity plotted in a log-log scale for the measured spectra M (open circle) and the F (filled triangle), X (filled diamond), and S (filled circle) bands.

size[10] (in Ref. 10, the sizes versus blueshifts were determined for $CsPbCl_3$ microcrystals embedded in CsCl crystals), and the mean crystallite size for the polycrystalline state was about 25 nm in diameter, which was measured by the x-ray diffraction method. Under high-power excitation, two new bands or structures show up. With the increase of excitation intensity, the microcrystalline state shows successive jumps of the dominant band, from the highest-energy free-exciton band to lower-energy new bands, while the polycrystalline state only exhibits less-resolved new structures. In particular, the third (lowest-energy) band in the microcrystalline state, abruptly appearing as a small peak for 44 kW/cm² excitation, grows rapidly with increasing excitation intensity.

The three bands for the microcrystalline state were always well resolved for every excitation intensity employed. Therefore, it was possible to apply spectral analyses to the bands. An example of the analysis is shown in Fig. 4, where the measured spectrum M for a 70 kW/cm² excitation is decomposed into three bands, namely, F (Lorentzian), X (Lorentzian), and S (Gaussian) bands. The F band is due to free-exciton emission, whose peak energy is very close to that of the free-exciton emission spectrum measured under low-power excitation (dashed curve in Fig. 2), and the X and S bands represent new emissions occurring under high-power excitation. Similar analyses were carried out for spectra mea-

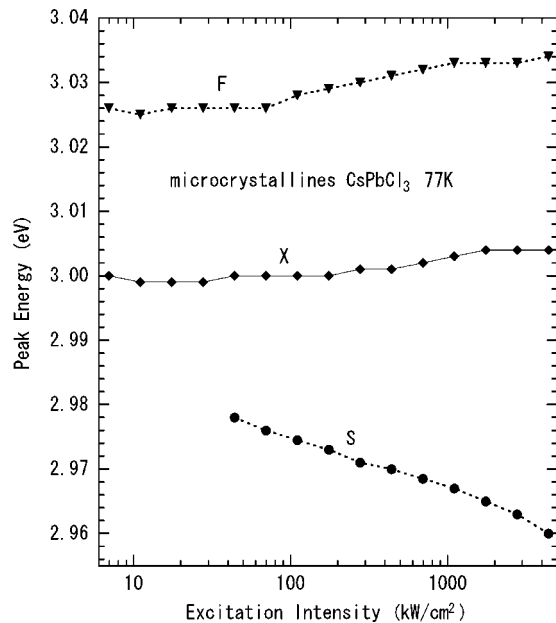FIG. 6. Peak energy versus excitation intensity plotted in a semi-log scale for the F (filled triangle), X (filled diamond), and S (filled circle) bands.
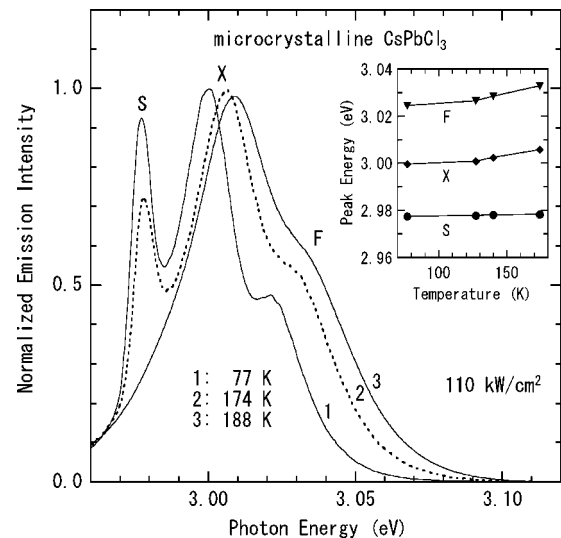

FIG. 7. Normalized luminescence spectra for the microcrystalline state of a film of 75 nm thickness with an effective crystallite diameter of 4.2 nm, measured under $110 \ kW/cm^2$ excitation as a function of temperature: curve 1 (77 K), curve 2 (174 K), and curve 3 (188 K). In the inset is shown the temperature dependence of the peak energies for the F (filled triangle), X (filled diamond), and S (filled circle) bands deduced by spectral analyses of the measured spectra.

range 1.2–0.9 for the measured spectrum M indicating that the total emission intensity increases nearly linearly with the excitation intensity throughout the whole range of the excitation intensity, roughly speaking. The F band also has nearly a constant slope throughout the whole range but showing a strongly sublinear dependence, with $n \sim 0.4$. On the other hand, different behaviors are exhibited for the new bands. The X band shows a linear dependence ($n \sim 1$) at low excitation intensities below $100 \ kW/cm^2$, and then changes to sublinear one ($n \sim 0.4$) above $200 \ kW/cm^2$. The S band, which appears abruptly at $40 \ kW/cm^2$ excitation, grows rapidly in the rage up to $100 \ kW/cm^2$ excitation showing a strongly superlinear dependence ($n \sim 2.9$), which is followed by a gradual change to a linear dependence at higher excitation intensities. We note that the total integrated emission intensity for the polycrystalline state also showed nearly a linear dependence on the excitation intensity throughout the whole range of the excitation intensity.

Concerning the peak energy versus excitation intensity, the F and X bands show similar behaviors. As the excitation intensity increases, both bands shift toward high energies (Fig. 6), with their energy separation (27–30 meV) almost unchanged. On the other hand, the S band shows redshift with increasing excitation intensity (Fig. 6). We note that the full width at half maximum (FWHM) of the band is very small at the initial stage of its growth, exhibiting a minimum of about 6 meV for $70 \ kW/cm^2$ excitation, as compared to those (>20 meV) for the F and X bands.

Figure 7 represents normalized luminescence spectra for $110 \ kW/cm^2$ excitation as a function of temperature of a microcrystalline film of 75 nm thickness with an effective crystallite diameter of 4.2 nm. The S band decreases in intensity with the rise of temperature and finally disappears at 188 K. The temperature at which the S band disappears was

shown to increase with increasing excitation intensity. As seen from the inset, where the peak energies of the F, X, and S bands deduced by spectral analyses are plotted versus temperature, the peak energy of the S band is almost unchanged with temperature. On the other hand, the F and X bands shift to high energies with the rise of temperature, but with their energy separation (26–27 meV) almost unchanged.

Figure 8 represents normalized luminescence spectra of a film of 73 nm thickness with the effective crystallite diameter of 4.4 nm, to show evolution of spectral line shape as a function of excitation intensity around which the S band starts to show up and subsequently grows in intensity. The exciting light was incident on the film at right angle and its spot at the film surface had a stripe shape with length about 5 mm and width less than 0.1 mm. The measurements were carried out for two different optical configurations, i.e., for film-edge scattering along the stripe length (solid curves) and for 45° backscattering with respect to the film plane (dashed curves). Although the spectra for the 45° backscattering show a similar behavior to those shown in Fig. 2, a characteristic behavior is exhibited for the film-edge scattering. The S band is already clearly observed at the lowest excitation power $6 \ kW/cm^2$ for the film-edge scattering, while for the 45° backscattering there is no trace of the S band at such a low excitation intensity. With increasing the excitation intensity, however, the spectral-shape difference between the two scatterings becomes small; indeed, above $100 \ kW/cm^2$ excitation, almost the same spectral shape was exhibited for the two scatterings (not shown in the figure). Similar measurements were carried out for a shorter excitation stripe, with the length about 1 mm (but with the same width); almost no changes in both spectral shape and spectral absolute intensity due to the reduction of the stripe length were recognized for
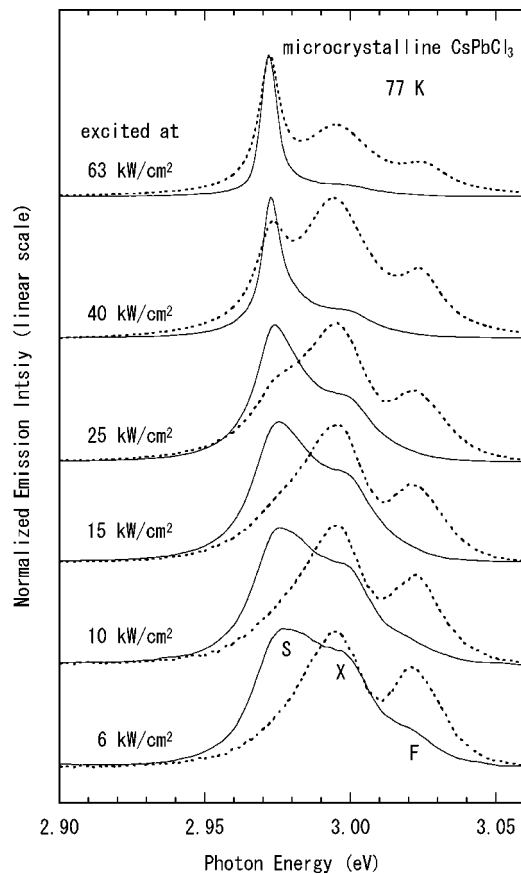
FIG. 8. Normalized luminescence spectra at 77 K of a film of 73 nm with an effective crystallite diameter of 4.4 nm, showing evolution of spectral line shape as a function of excitation intensity around which the S band starts to show up and subsequently grows in intensity. The spectra were measured for the film-edge scattering (solid curves) and 45° backscattering (dashed curves), see the text.

the film-edge scattering, while for the backscattering the spectra were reduced in absolute intensity by a factor of about 5 without showing any change in spectral shape (except reduced signal-to-noise ratio in the spectra).

IV. DISCUSSION

The luminescence spectra of the highly-excited $CsPbCl_3$ films are very different in feature from those of bulk crystals. Baltog *et al.*[9] measured luminescence spectra of $CsPbCl_3$ bulk single crystals at 77 K under high-power N_2 laser-light excitation. They found, in total, five new emission bands, namely, E_i bands with i ranging from 1 to 5 in the order of decreasing photon energy, for excitation intensities up to 400 kW/cm². The E_1, E_2, E_3, and E_5 bands were associated with phonon replicas of the free exciton. The E_4 band, locating at around 2.97 eV for 400 kW/cm² excitation, was assigned as due to an exciton-electron inelastic collision process. As compared with this rather complicated luminescence behavior of the bulk single crystals, the emission spectra for the present films only compose of three bands, although different outlines are exhibited for the spectra according as the films are in the microcrystallline (Fig. 2) or polycrystalline

(Fig. 3) state. In what follows we will mainly discuss the luminescence behavior for the microcrystalline state, for which the three bands are nicely decomposed as shown in Sec. III.

We first consider the origin of the X band. A hint may be given by noting the fact that, with increasing the excitation intensity, the peak energy of the band shifts almost in parallel with that of the F band as seen from Fig. 6. This suggests that the X band is a phonon replica of the F band. This is consistent with the fact that the energy spacing of the two bands is almost unchanged against the rise of temperature (Fig. 7, inset). The value of the energy spacing 27–30 meV (Fig. 6) in the whole range of the excitation intensity, is close the phonon energy of 25 meV reported in Ref. 11, where twelve Raman active phonons were resolved at 77 K for bulk single crystals of $CsPbCl_3$. In the abovementioned luminescence spectra of bulk $CsPbCl_3$ crystals, the same phonon (of 25 meV energy) is related to the E_2 band.

On the other hand, the S band shows characteristic dependence on excitation intensity. The peak energy of the band decreases with increasing excitation intensity (Fig. 6), similar to the case for the E_4 band of bulk $CsPbCl_3$ crystals. In the exciton-electron inelastic collision process,[12] to which the E_4 band has been attributed as mentioned above, the exciton is radiatively dissociated transferring a fraction of its energy to the electron. The transferred energy increases with increasing excitation intensity. As a result, the peak energy of the luminescence decreases with increasing excitation intensity, starting from the highest, free-exciton peak energy, for low-power excitations, to lower energies, for high-power excitations. In the case of the S band, however, its peak energy is already smaller, by about 48 meV, than the free-exciton peak energy (F-band energy) even for the lowest excitation intensity (44 kW/cm²) at which the S band starts to show up. Such a characteristic behavior of the S band may be explained in terms of exciton-exciton inelastic collision.[12] In the collision process of two $n=1$ excitons, one exciton is scattered into a high-energy exciton state with $n \geqq 2$, while the other exciton is scattered into a photonlike state escaping as a luminescence photon of energy more than $(3/4)E_b$ lower than that of the free-exciton luminescence, where E_b is the binding energy of the free exciton. From the relation $(3/4)E_b = 48$ meV for the S band observed at the lowest excitation intensity, we obtain $E_b = 64$ meV, which is comparable to the reported free-exciton binding energies of $CsPbCl_3$, 60–67 meV.[13–15] Therefore, the S band can be attributed to exciton-exciton inelastic collision, and the red shifts of the band at the higher excitation intensities should be explained in terms of a general relation of the form[12]

$$E_S = E_F - E_b(1 - 1/n^2) - 3\delta k_B T_{eff}, \quad n = 2, 3, \ldots, \quad (1)$$

where E_S and E_F are the energies of the luminescence photon and the free exciton, respectvely, δ is a positive constant smaller than 1, and T_{eff} is the effective temperature. According to Eq. (1), there are two possible causes for the redshift: one is related to T_{eff}, which increases with increasing excitation intensity, and the other is the change in the n value, from $n=2$ to higher ones including infinity ($n=\infty$). In view of the large values of the redshift, as large as 18 meV (for the

highest excitation intensity), which is even larger than $(1/4)E_b \sim 16$ meV, the change in the n value is considered to be the dominant cause for the redshift. In particular, the change from $n=2$ (P_2 emission) to $n=\infty$ (P_∞ emission) may be the most probable, in analogy with the case for ZnO (Ref. 16) ($E_b=60$ meV), where the P_2 emission occurring at low excitation levels (<20 kW/cm^2 at 1.9 K) is quickly overwhelmed by the P_∞ emission at higher excitation levels. The unresolved feature of the two emissions for the S band is considered to be due to the size distribution of the microcrystallites in the films.

The above attribution of the X and S bands leads to the following picture of the role of free excitons in the luminescence. The free excitons created under high-power excitation are in a thermal nonequilibrium distribution, with the effective temperature higher than the lattice temperature. The "energetic" excitons can interact with phonons and with each other. The dominant interaction is exciton-phonon inelastic collision at intermediate densities of the excitons and exciton-exciton inelastic collision at higher densities, yielding the X and S bands, respectively. The jumping between the two interactions occurs at excitation intensities near 200 kW/cm^2 (Figs. 2 and 5).

Concerning the luminescence intensities associated with exciton-exciton inelastic collision, theory predicts that the integrated luminescence intensity I_{em} versus excitation power I_{ex} is expressed by a power relation of the form of $I_{em} \propto I_{ex}^n$ with $n=2$.[12] The slope n for the S band shown in Fig. 5 is 2.9 in the range 40 kW/cm$^2 < I_{ex} < 100$ kW/cm^2, which exceeds the theoretical value of 2. This suggests the occurrence of stimulated emission. The very small FWHM of the band, about 6 meV at 70 kW/cm^2 excitation, is favorable for the assumption of stimulated emission. Such a tendency of stimulated emission is more clearly seen in Fig. 8. Spectral analyses for the film-edge emission (solid curves) showed that the value of n in the expression $I_{em} \propto I_{ex}^n$ for the S band amounted to 3.6 in the I_{ex} range of 40-60 kW/cm^2 and that the narrowing of the band started to occur at 10 kW/cm^2 showing the smallest FWHM, 5.5 meV, at 60 kW/cm^2.

A further information about the stimulated emission can be obtained from a careful inspection of Fig. 5. That is, the stimulated emission for the S band contributes to a rather superlinear increase of the total emission intensity (curve M) and does not suppress the intensity of the main band (X band). After the jumping of the main band (from X to S), however, the slope n for the S band decreases toward the values even smaller than 2, the theoretical value, due to saturation effects. This accompanies the increase of FWHM of the band (Fig. 2).

Baltog *et al.*[9] demonstrated that the E_4 band observed for bulk single crystals of CsPbCl$_3$ shows a behavior of stimulated emission for a particular scattering optical configuration. They irradiated the crystals at 77 K with an N$_2$ laser and measured the luminescence spectrum in a detection configuration in which the angle ϕ between the emitted light and the irradiated crystal surface was very small, about 9°. At excitation powers above 100 kW/cm^2, stimulated emission was observed for the E_4 band, peaking at around 2.966 eV. However, it was difficult to observe stimulated emission for $\phi \sim 45°$. A long optical path within the irradiated crystals

was necessary for the stimulated emission to occur in the crystals, in great contrast to the case of the present microcrystalline films.

In the microcrystalline films, since the stimulated emission for the S band is observed even for the perpendicular-to-film emission, a very short optical gain length is expected. As seen from Fig. 8, when the luminescence is measured for scattering in the direction along the long optical path (film-edge scattering along the stripe length), the S band is already enhanced by a gain mechanism at a very low excitation intensity as low as 6 kW/cm^2, while showing the band narrowing at higher excitation intensities. On the other hand, in the direction along the short optical path (45° backscattering), the S band starts to show up at higher excitation intensities around 25 kW/cm^2 and subsequently grows rapidly with increasing excitation intensity due to the effect of light amplification. We note that, at high excitation intensities above 100 kW/cm^2, the difference in the spectral shape between the two scatterings became very small as mentioned in Sec. III. This is considered to be due to the effect of saturation, which may occur within a very short optical path length, of stimulated emission, suggesting a very short gain length for the stimulated emission. On the other hand, at low excitation intensities (below 100 kW/cm^2), a saturation of optical amplification is considered to occur within a mm length, because almost no changes in both spectral shape and spectral absolute intensity due to the reduction of the stripe length from 5 to 1 mm were recognized for the film-edge scattering, as mentioned in Sec. III. Therefore, at any excitation intensity, light amplification due to net gain over a mm-scale distance is not attainable due to self-absorption; instead, at sufficiently high excitation intensities, large optical amplification due to large net gain may be achieved within a very short gain length.

Presumably, the large-gain mechanism is attributed to excitonic superradiance, which, as mentioned in Sec. I, has been observed for microcrystalline films prepared in the same way. So far, possible evidence of mesoscopic enhancement of optical gain due to the effect of exciton giant oscillator strength on the stimulated emission has been reported only for epitaxy-grown microcrystalline ZnO films,[17,18] which are a promising wide-band-gap high-gain medium for short wavelength semiconductor lasers as now recognized by many workers.[19] The microcrystalline CsPbCl$_3$ films may provide an inexpensive high-gain medium for short wavelength semiconductor lasers due to ease of the film preparation method. We are in progress of developing photoexcited Fabry-Perot vertical-microcavity lasers (thin-film lasers), in which single-mode lasing across the film thickness occurs.

V. CONCLUSION

Photoluminescence of CsPbCl$_3$, which is known to be one of the most photoluminescent semiconductors, and for which we previously reported that thin films prepared in the form of microcrystalline/polycrystalline states via the amorphous phase by crystallization exhibit more than an order of magnitude stronger free-exciton emission due to excitonic superradiance for the microcrystalline state than for the polycrys-

talline state, but with even the latter state still being characterized by stronger free-exciton emission than bulk single crystals, has been measured under high-power excitation for thin films prepared in the same way. Unlike the case for bulk single crystals, where five new emission bands are known to occur under high-power excitation, only two new bands occur for the thin films. With the increase of excitation intensity, the microcrystalline state of the films shows successive jumps of the dominant band, from the highest-energy free-exciton band (F band) to the lower-energy X band and finally to the lowest-energy S band, while the polycrystalline state only exhibits less-resolved, three corresponding structures. The X band is assigned as a phonon replica of the F band and the S band is attributed to exciton-exciton inelastic collision. The S band shows behaviors characteristic of stimulated emission (spectral narrowing; superlinearity in the expression $I_{em} \propto I_{ex}^n$, with n larger than the theoretically expected value, 2, for exciton-exciton inelastic collision). The stimulated emission is observed even for single path light amplification in the direction perpendicular to the films (film thickness, of order 80 nm) indicating a very short gain length, unlike in the case of bulk single crystals, where stimulated emission is known to occur only for a particular, long-gain-length geometry. The expected, very large optical gain for the microcrystalline state of the films is attributable to giant oscillator strength effect characteristic of excitonic superradiance.

*Electronic address: d930963@icpc00.icpc.fukui-u.ac.jp

[1] See, for example, H. G. Gottwald, T. Lieser, K. G. Weil, and A. Weiss, Z. Naturforsch. Teil A **40**, 677 (1985).

[2] See, for example, S. Kondo, T. Itoh, S. Saito, and M. Mekata, Solid State Commun. **78**, 557 (1991).

[3] See, for example, H. G. Gottwald and K. G. Weil, Ber. Bunsenges. Phys. Chem. **92**, 60 (1988).

[4] See, for example, S. Kondo, T. Sakai, H. Tanaka, and T. Saito, Phys. Rev. B **58**, 11401 (1998).

[5] See, for example, S. Kondo, S. Kagawa, and T. Saito, Phys. Status Solidi B **154**, 583 (1996).

[6] See, for example, S. Kondo, K. Amaya, and T. Saito, Mater. Sci. Eng., B **88**, 85 (2001).

[7] B. A. Belikovich, I. P. Pashchuk, and N. S. Pidzyrailo, Opt. Spectrosc. **42**, 62 (1977).

[8] S. Kondo, H. Nakagawa, T. Saito, and H. Asada, J. Phys.: Condens. Matter **15**, 1247 (2003).

[9] Baltog, L. Mihut, and S. Lefrant, J. Lumin. **68**, 271 (1996).

[10] M. Nikl, K. Nitsch, K. Polak, E. Mihokova, S. Zazubovich, G. P. Pazzi, P. Fabeni, L. Salvini, R. Aceves, M. Barbosa-Flores, R. Perez Salas, M. Gurioli, and A. Scacco, J. Lumin. **72–74**, 377 (1997).

[11] D. M. Calistru, L. Mihut, S. Lefrant, and I. Baltog, J. Appl. Phys. **82**, 5391 (1997).

[12] C. Klingshirn, Phys. Status Solidi B **71**, 547 (1975).

[13] D. Fröhlich, K. Heiderigh, H. Kunzel, G. Trendel, and J. Treusch, J. Lumin. **18/19**, 385 (1979).

[14] I. P. Pashuk, N. S. Pidzyrailo, and M. G. Matsko, Sov. Phys. Solid State **23**, 1263 (1981).

[15] S. Kondo, H. Mori, and T. Saito, Phys. Status Solidi A **163**, 445 (1997).

[16] J. M. Hvam, Phys. Status Solidi B **63**, 511 (1974).

[17] M. Kawasaki, A. Ohtomo, I. Ohkubo, H. Koinuma, Z. K. Tang, P. Yu, G. K. L. Wong, B. P. Zhang, and Y. Segawa, Mater. Sci. Eng., B **56**, 239 (1998).

[18] P. Zu, Z. K. Tang, G. K. L. Wong, M. Kawasaki, A. Ohtomo, H. Koinuma, and Y. Segawa, Solid State Commun. **103**, 459 (1997).

[19] See, for example, S. F. Yu, C. Yuen, S. P. Lau, Y. G. Wang, H. W. Lee, and B. K. Tay, Appl. Phys. Lett. **83**, 4288 (2003).